Structural Features of *meso*-Tetrakis(4-carboxyphenyl)porphyrin Interacting with Amino-Terminated Poly(propylene oxide)

Maria Angela Castriciano,[†] Andrea Romeo,[†] Nicola Angelini,[‡] Norberto Micali,[‡] Alessandro Longo,[§] Antonino Mazzaglia,[⊥] and Luigi Monsù Scolaro*,[†]

Dipartimento di Chimica Inorganica, Chimica Analitica e Chimica Fisica, and C.I.R.C.M.S.B., Università di Messina, Salita Sperone 31, 98166 Vill. S. Agata, Messina, Italy; IPCF-CNR, Via La Farina 237, 98123, Messina, Italy; ISMN-CNR, Via Ugo La Malfa 153, 90146 Palermo, Italy; and ISMN-CNR, Salita Sperone 31, 98166 Vill. S. Agata, Messina, Italy

Received March 15, 2006; Revised Manuscript Received May 27, 2006

ABSTRACT: The neutralization reaction between the *meso*-tetrakis(4-carboxyphenyl)porphyrin (TPPC) and *O*-(2-aminopropyl)-*O*′-(2-methoxyethyl)poly(propylene glycol) (Jeffamine M-600) in 1:4 stoichiometric ratio affords a stable supramolecular adduct (TPPC@Jeffamine). This species has been characterized in aqueous and chloroform solution through a series of spectroscopic techniques, including ^{1}H and ^{13}C NMR spectroscopy, UV/vis absorption, steady-state and time-resolved fluorescence emission, time-resolved fluorescence anisotropy, and resonance light scattering. All the experimental findings point to a different structural arrangement of the porphyrin chromophores within the supramolecular adduct depending on the quality of the solvent. In aqueous solution, the TPPC@Jeffamine contains mainly monomeric porphyrins while the flexible polymeric chains are folded and entangled to give larger aggregates. An insight into the structure of the basic building unit is given by SAXS measurements which, assuming a core−shell model, afford an internal core radius $R_1 = 15.3$ Å and an external radius $R_2 = 21.8$ Å, in line with the expected dimension of the single unit, based on a single porphyrin surrounded by four Jeffamine chains. In chloroform, the adduct rearranges and porphyrins oligomers are stabilized by ion-pairing with Jeffamine, which, due to its hydrophobic nature, swells in this solvent.

Introduction

Porphyrins are an important class of natural and artificial pigments which play an important role in largely different area of both fundamental and technological interest. In particular, porphyrins bearing hydrophilic pendant groups conferring water solubility have received special attention because their metal derivatives have been exploited as models for enzymes[1,2] and artificial blood.[3] Charged porphyrins are able to interact with several relevant biomolecules, i.e., nucleic acids,[4−8] polypeptides,[9−15] and proteins.[16,17] This property together with their ability to localize into tumor cells and to photosensitize the production of singlet oxygen led to the development of several compounds actually in use or under investigation for photodynamic therapy applications (PDT).[18] A common feature of these molecules is their propensity to interact to form dimers, oligomers, or more extended aggregates.[19] The extent of self-aggregation can be controlled by a series of factors, including the nature of the specific porphyrin (substituent groups and coordinated metal ion) and environmental changes (pH, ionic strength, cosolvents, temperature, etc.).[20−23] It is important to note that many of the physicochemical properties of this class of pigments, and in particular the electronic absorption and the luminescence, are strictly dependent on their aggregation state. For example, the B-band (Soret band) and the Q-bands, which are the main absorption features for these dyes in the near-UV and visible range, respectively, exhibit different changes depending on the geometrical arrangement between the chromophores: (i) an hypsochromic shift is related to the formation of H-type aggregates (face-to-face) while (ii) a bathochromic shift is associated with J-type aggregates (side-by-side).[24,25] Another consequence of porphyrin aggregation is the quenching of their fluorescence emission, very often related to the consistent decrease of the fluorescence lifetime of the corresponding excited states.

Among the anionic porphyrins, the *meso*-tetrakis(4-sulfonatophenyl)porphyrin (TPPS) has been largely investigated because of its tendency to self-assemble at acidic pH and in the presence of a variety of simple cationic species forming extended J-aggregates,[26−34] which exhibit interesting nonlinear optical[35] and optoelectronic properties.[36] Despite this large amount of reports on TPPS, much less attention has been devoted to the *meso*-tetrakis(4-carboxyphenyl)porphyrin (TPPC). At difference with TPPS, whose peripheral sulfonate groups remain unprotonated up to very acidic conditions, the carboxylate groups in TPPC are easily neutralized in the range of pH 5−7 (the highest pK_a value is 6.6),[37] leading to a neutral species which is scarcely soluble in aqueous solutions. At pH <1 the nitrogen atoms of the porphine core get protonated, yielding a dicationic porphyrin which is able to self-assemble into J-aggregates, whose exciton spectra exhibit wavelength dependence on the counteranion nature.[38,39] Under neutral conditions, TPPC is a monomer only at very low concentration (<2 μM) and at low ionic strength, while it tends to dimerize on increasing the ionic strength. In the presence of 0.1 M KNO_3 at pH 7.5 a value of 4.55×10^4 M^{-1} has been determined for the dimerization equilibrium constant from the analysis of the absorbance data.[40] H-type aggregates have been investigated in aqueous solutions at pH ∼3.5, and an average size of 15−20 Å has been calculated on the basis of time-resolved fluorescence anisotropy experiments.[41] A distribution of species has been also reported in micellar and premicellar systems made by both ionic and nonionic surfactants.[42] Solvatochromic and specific solute

[†] Università di Messina.
[‡] IPCF-CNR.
[§] ISMN-CNR.
[⊥] ISMN-CNR.
* Corresponding author: Ph +39 090 6765711; Fax +39 090 393756; e-mail lmonsu@unime.it.

10.1021/ma060583i CCC: $33.50
Published on Web 07/06/2006

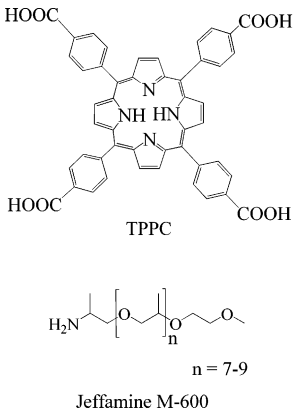

Figure 1. Molecular formulas of TPPC and Jeffamine M-600.

effects have been pointed out for this porphyrin: the position of the Soret band and the molar extinction coefficient can change in the range 408−419 nm and (3.9−5.1) × 10^5 M^{-1} cm^{-1}, respectively, depending on the nature of the solvents and the added electrolyte, with a blue shift in more polar environments.[37] Formation of aggregated species on titanium dioxide[43] and stable 1:1 and 1:2 complexes with various viologens[37] have been also reported.

Interestingly, quite recently, TPPC has been exploited as a marker for the rapid detection of tumor cells by fluorescence imaging.[44] To develop efficient systems for biomedical applications or for PDT (in which aggregation should be prevented) or to stabilize monomeric porphyrins in an very water-soluble form, novel systems based on biocompatible delivery systems are highly desirable.

Amino-terminated polypropylene or poly(ethylene oxide)s are generally termed as Jeffamines and can have linear or branched chains terminated with ionizable amino groups. These polymers are biocompatible and can be easily grafted with other polymers[45,46] to obtain stimulus responsive drug delivery systems[47] or to prepare dispersions in which Jeffamine acts as costabilizer.[48] Jeffamine-containing copolymers have been also investigated for blood compatibility of poly(ether urethane)s,[49] in the reduction of aortic wall calcification,[50] and for systems able to haemolyse the erythrocyte membrane.[51] These polymers find also application in protein crystallization[52] or in enzyme immobilization.[53] Furthermore, this class of molecules have been largely exploited in materials preparation and applications.[54−59]

Here we report on the formation and structural characterization through a variety of spectroscopic techniques of a supramolecular complex between the TPPC porphyrin and an amino-terminated poly(propylene glycol) (Jeffamine M-600) (Figure 1). We anticipate that electrostatic attractive forces drive the interaction between the deprotonated carboxylic groups of TPPC and the protonated primary amino groups of the polymer, affording a remarkably stable adduct. The polymeric chains actually prevent porphyrin aggregation, allowing to reach millimolar concentration of TPPC in a monomeric form. Because of the amphiphilic nature of Jeffamine, large structural changes occur on varying the quality of the solvent.

Experimental Section

Materials. The porphyrin *meso*-tetrakis(4-carboxyphenyl)porphyrin (TPPC) and *O*-(2-aminopropyl)-*O*′-(2-methoxyethyl)poly(propylene glycol) (Jeffamine M-600), average FW ∼ 600, were purchased from Aldrich Co. All solvents were reagent grade, available from commercial suppliers (Analytical Reagent Grade, Lab-Scan Ltd.). Chloroform-*d* (99.8+%, C.I.L. Inc.) and D_2O (99.9+%, Aldrich Co.) were used as received.

The supramolecular adduct between TPPC and Jeffamine (TPPC@Jeffamine) has been prepared by mixing 160 mg (0.2 mmol) of solid porphyrin (tetracarboxylic acid) with 490 mg (0.8 mmol) of the liquid polymer. The resulting mixture has been amalgamated in order to make it as homogeneous as possible. The product has been suspended in chloroform, stirred at room temperature for about 4 h, and then dried under vacuum, affording a waxy dark red solid. Aqueous stock solutions (10 mM phosphate buffer pH 7) of this compound were prepared in dust-free Millipore water and stored in the dark. ^{1}H NMR (D_2O): δ 8.54 (br s, 8H), 8.24 (d, 8H), 7.76 (d, 8H), 3.74−2.92 (m, 147H), 1.20−0.54 (m, 120H). $^{13}C\{^1H\}$ NMR (D_2O): δ 176 (C_{quat}), 145.7 (C_{quat}), 139 (C_{quat}), 136.8 (CH), 132 (CH), 131.2 (CH), 130.5 (CH), 122 (C_{quat}), 78−77 (CH), 76.6−72 (CH_2), 60.6−49.5 (CH), 19.7−16.8 (CH_3). UV−vis (water): (λ_{max}/nm) 416 ($\epsilon = 3.94 \times 10^5$ M^{-1} cm^{-1}), 522, 562, 592, 652; ($CHCl_3$): (λ_{max}/nm) 410, 430, 520, 554, 596, 650. Fluorescence emission (water): (λ_{exc}/nm) = 430, (λ_{em}/nm) = 650, 712; ($CHCl_3$): (λ_{exc}/nm) = 430, (λ_{em}/nm) = 650, 714.

Methods. ^{1}H and $^{13}C\{^1H\}$ NMR spectra were recorded at 298 K on a Bruker AMX R-300 spectrometer operating with a broad-band probe at 300.13 and 75.7 MHz for ^{1}H and ^{13}C nuclei, respectively. Chemical shifts are reported in ppm downfield from $SiMe_4$, with respect to dioxane as internal standard. The ^{13}C signals have been assigned through standard DEPT sequence. UV/vis spectra were obtained on a Hewlett-Packard model 8453 diode array spectrophotometer using 0.001−1 cm path length quartz cells. Luminescence and resonance light scattering (RLS) spectra were recorded on a Jasco FP-750 spectrofluorimeter equipped with a Hamamatsu R928 phototube adopting a synchronous scan protocol for RLS experiments.[60] The emission spectra were not corrected for the absorption of the samples. All the other fluorescence measurements were carried out by a time-correlated-single-photon-counting (TCSPC)[61] homemade apparatus (λ_{ex} = 575 nm), which has been already described.[62] The fluorescence decay profiles were analyzed through a nonlinear least-squares iterative deconvolution procedures based on the Marquardt algorithm,[63] achieving an instrumental resolution of about few tens of picoseconds. The total fluorescence decay curves were fitted to a multiexponential decay equation:[64]

$$I(t) = I_0 \sum_i \alpha_i \exp(-t/\tau_i) \tag{1}$$

where $I(t)$ is total fluorescence decay curve, I_0 is the intensity at $t = 0$, and α_i and τ_i are relative amplitude and lifetime of ith component (the normalization condition being $\sum_i \alpha_i = 1$), respectively. Fluorescence anisotropy, $r(t)$, is defined according to the following equation:

$$r(t) = \frac{I_{VV}(t) - I_{VH}(t)}{I_{VV}(t) + 2I_{VH}(t)} \tag{2}$$

where VV and VH indicate respectively the vertically and horizontally polarized emission, being the excitation beam vertically polarized. Since, in our experimental conditions, the anisotropy decay times were much longer than the overall instrumental response (∼200 ps), no deconvolution procedure was applied, and the $r(t)$ curves were simply fitted to the following exponential decay equation:

$$r(t) = r_0 \exp(-t/\tau_R) \tag{3}$$

where r_0 is the fundamental anisotropy and τ_R the rotational correlation time. Assuming a simple case of "spherical molecules", τ_R is related to the volume V of the equivalent sphere by

$$\tau_R = \frac{\eta V}{k_B T} \tag{4}$$

with η the microviscosity of the medium, T the temperature in kelvin, and k_B the Boltzmann constant.

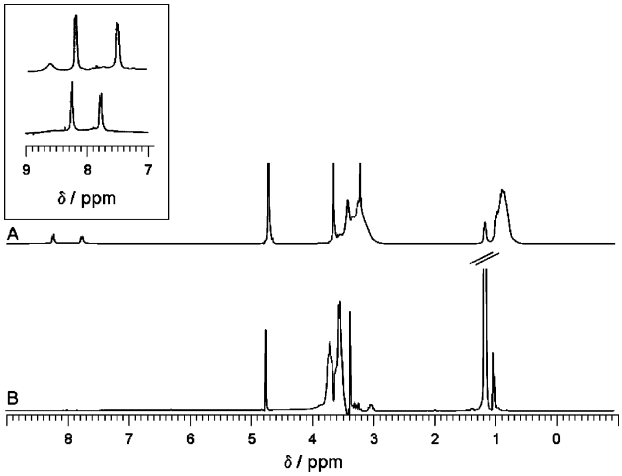

Figure 2. ^{1}H NMR spectra of TPPC@Jeffamine complex (A) and Jeffamine (B) in D_2O at 298 K. The inset shows an expansion of the aromatic region for the parent TPPC sodium salt (upper plot) and the TPPC@Jeffamine system (lower plot).

Small-angle X-ray scattering (SAXS) patterns have been recorded by a laboratory instrumentation consisting of a Philips PW X-ray generator (providing Cu Kα, Ni-filtered X-ray radiation, $\lambda = 1.5418$ Å) with a Kratky-type small-angle camera in the "finite slit height geometry" equipped with step scanning motor and scintillation counter as detector. The range of scattering vector covered is 0.005 Å^{-1} < q < 0.6 Å^{-1}. All measurements were carried out at 298 K. The scattering data were normalized with respect to transmission and corrected by contributions due to the empty cell and solvent. Best-fit analyses were performed using homemade programs based on the CERN minimization procedure MINUITS. The smearing effect, due to instrumental setup, was taken into account during the minimization of the data according to a standard procedure.[65−67]

Results and Discussion

The adduct between TPPC and Jeffamine can be easily prepared by a one-pot acid−base reaction between a known amount of solid porphyrin with the liquid polymer in a 1:4 stoichiometric ratio. The resulting supramolecular species is extremely soluble in water, where it remains stable for months, as confirmed by the invariance of UV/vis and ^{1}H NMR spectra. The structure is mainly stabilized through electrostatic interactions acting between the anionic carboxylate groups of the porphyrin and the charged protonated amino groups of the polymer. The nature of the interaction between the two constituting molecular components is supported by the effect of increasing the ionic strength (>10 mM) or lowering the pH (<5): the formation of a turbid solution is a clear indication of disruption of the adduct with partial or extensive aggregation and precipitation of the porphyrin. For these reasons, the system has been characterized both in neutral and at low ionic strength aqueous solutions and in chloroform solutions through a combination of different spectroscopic techniques.

NMR Spectroscopy. The ^{1}H NMR spectrum of the adduct in D_2O displays doublets centered at δ 8.24 and 7.76 ppm due to the ortho and meta protons, respectively, of the peripheral meso phenyl substituent groups on the porphyrin ring (Figure 2). A very broad peak can be detected at δ 8.54 ppm corresponding to the β-pyrrole protons. The broadening of this latter resonance can be probably ascribed to a tautomeric equilibrium slow in the NMR time scale of the inner N−D groups of the porphine core.[68] Accordingly, variable temperature NMR experiments show that this signal sharpens on increasing the temperature up to 312 K, while it is still not resolved even at 273 K (data not shown). All the resonances belonging to the porphyrin are shifted downfield with respect to the corresponding sodium salt of the parent porphyrin (inset of Figure 2). The aliphatic region of the ^{1}H NMR spectrum shows peaks in the range δ 3.74−2.92 ppm and δ 1.35−0.82 ppm, corresponding respectively to CH, CH_2 and CH_3 protons of the Jeffamine polymer. An exact assignment of the various resonances in this region is prevented by the polydispersivity of the starting polymer. Anyway, a general downfield shift of all the peaks with respect to the signals of the free polymer, due to the ring current of the porphyrin ring, is clearly evident. Furthermore, the signals of the protons belonging to the aliphatic chain, and in particular the resonance of the terminal methyl group (δ 0.98 ppm) close to the amino moiety, are broadened in the adduct in comparison to the free polymer. This evidence suggest an increase in the molecular mass and a slowing down of the molecular tumbling in solution, with a concomitant decrease of the relaxation times. The ^{13}C NMR spectrum has been tentatively assigned by standard DEPT sequence and by comparison with the spectra of the free polymer and porphyrin sodium salt. In the aromatic region, all the signals relative to the porphyrin appear slightly upfield shifted with respect to TPPC. The aliphatic region exhibits the presence of the resonances for the carbon atoms of the polymer chain, and also in this case a general upfield shift in comparison with the free Jeffamine is well evident. In particular, the signal at δ 18 ppm assigned to the terminal methyl groups undergoes to an upfield shift ~3 ppm. A downfield shift (~2 ppm) is evident for the CH_2 group at about δ 49 ppm due to the presence of the neighbor amino group.

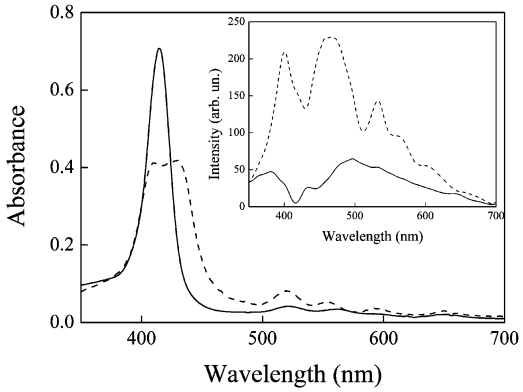

Figure 3. UV/vis spectra of 2 μM solutions of TPPC@Jeffamine in aqueous solution (solid line) and in chloroform solution (dashed line) at 298 K. The inset shows the corresponding RLS spectra in aqueous solution (solid line) and in chloroform solution (dashed line).

UV/Vis Absorption, Steady-State Fluorescence, and Resonance Light Scattering. The UV/vis spectrum of the TPPC porphyrin (sodium salt) in aqueous solution at pH 7 displays a B-band located at 414 nm accompanied by four Q-bands at 516, 533, 580, and 635 nm, exhibiting the so-called etio pattern.[69] In the supramolecular complex, the B-band is bathochromically shifted with respect to TPPC sodium salt ($\Delta\lambda = +2$ nm, $\epsilon = 3.94 \times 10^5$ M^{-1} cm^{-1}) and similarly the four Q-bands at longer wavelengths (522, 562, 592, and 652 nm) (Figure 3). The presence of the four Q-bands indicates that the core of the TPPC ring is unprotonated and retains the D_{2h} symmetry typical of the free base porphyrin.[42] Even if this porphyrin exhibits a strong dependence of the absorption features on the medium properties, it is interesting to note that the position of the Soret band in the adduct is similar to that already reported in concentrated aqueous solution of tetramethylammonium perchlorate. This shift has been suggested as indicative of a more organic environment around the porphyrin.[37] As mentioned above, the supramolecular

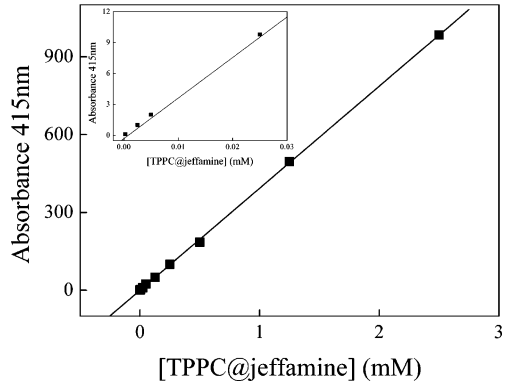

Figure 4. Beer law on the TPPC@Jeffamine adduct in aqueous solution. The inset reports an expansion of the low concentration range (cell path length 0.001−1 cm).

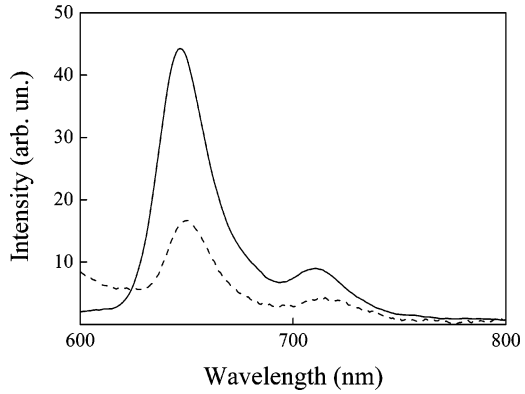

Figure 5. Fluorescence emission spectra of 2 μM solutions of TPPC@Jeffamine in aqueous solution (solid line) and in chloroform solution (dashed line) (λ_{exc} = 430 nm) at 298 K. The intensity emission of the sample in chloroform solution is multiply by a factor 100.

adduct is soluble in aqueous solution up to millimolar concentration (60−80 mM), whereas the parent porphyrin (TPPC) is only slightly soluble (<50 μM).[42] Furthermore, the Beer law for the adduct is hold up to 3 mM (Figure 4), suggesting that, under our experimental conditions, (i) no aggregation of the porphyrin chromophores is occurring, (ii) the adduct behaves as a stable compound, and (iii) no acid−base equilibria seem to be operative.

The monomeric nature of this species is strongly supported by the RLS profile which is only slightly larger than the neat solvent and shows a well corresponding to the B-band, due to photon loss for absorption (solid line, inset of Figure 3). The system is strongly emissive in aqueous solutions, and fluorescence spectra display the typical two banded pattern very similar to those of the parent porphyrin and of other tetraaryl-substituted porphyrins (Figure 5). The emission features at 650 and 712 nm are blue-shifted ($\Delta\lambda$ = −10 nm) with respect to the tetraanionic TPPC porphyrin.[42]

Dramatic changes are observed in the spectroscopic behavior of this system in chloroform solution, in line with the reported solvatochromic properties of TPPC.[37] In this organic solvent, the Soret band appears split with two components centered at 410 and 430 nm, respectively. A similar broaden and shifted B-band has been reported in the case of TPPC aggregates in mild acidic aqueous solutions.[41] The corresponding fluorescence emission spectrum shows a substantial quenching and a modest bathochromic shift of the two bands with respect to the same sample in water solution. The RLS spectrum shows the presence of a rather large Rayleigh scattered light component, modulated by absorption of the sample, without any specific resonance

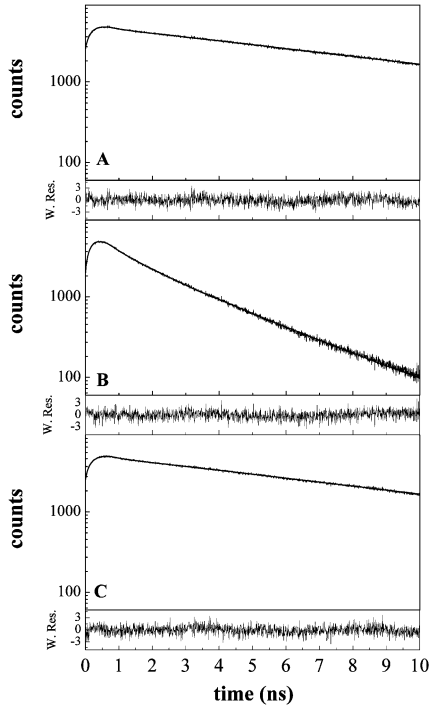

Figure 6. Fluorescence decays of (A) TPPC sodium salt in aqueous solution and (B) TPPC@Jeffamine in chloroform solution and in (C) aqueous solution at 298 K, together with the fit curves (the straight lines) and the weighted residuals.

peak (dashed line, inset of Figure 3). All these spectroscopic evidences point to the occurrence of small porphyrin aggregates in these samples. The RLS phenomenon is an enhancement of the scattered light intensity in the red edge of an absorption band, which is related to the extent of electronic coupling between adjacent chromophores, to the molar extinction of the individual chromophores and to the size and the geometry of the aggregates.[60] According to the RLS theory, the absence of any resonance peak indicates that only a small number of interacting chromophores (n < 25) should be involved in the structural arrangement of our system in chloroform solution.[70]

Time-Resolved Fluorescence. Time-resolved fluorescence measurements were performed at 298 K on sodium salt of TPPC in aqueous solution and on the supramolecular adduct in both chloroform and aqueous solution. In the latter case the fluorescence lifetimes were measured also at 323 K. Typical fluorescence decay curves for these systems are shown in Figure 6 (together with their weighted residuals to evaluate the goodness of the fit). The emission decays of TPPC sodium salt in aqueous solution (trace A) and the adduct (trace C) show a biexponential behavior with similar lifetime values (8.5 and ∼0.3 ns), but with different relative amplitudes (21% and 79% vs 46% and 54%, in the absence and in the presence of Jeffamine, respectively).

At 323 K in aqueous solutions, the longest lifetime value in the adduct decreases to 7.9 ns, whereas the shortest one increases to 1.2 ns, being the relative amplitudes about the same. Actually, the fluorescence emission of the long-living form, as expected, is "temperature-quenched" (through dynamic quenching), whereas the shortest fluorescent component is "temperature-enhanced". In this latter case, the emission behavior is compatible to the temperature effects on the static fluorescence quenching due to an aggregation process of fluorescent molecules.[64] On increasing the temperature, the aggregation process (and consequently the static quenching) is disfavored and the fluorescence emission is enhanced. On these bases the long-living fluorescent species

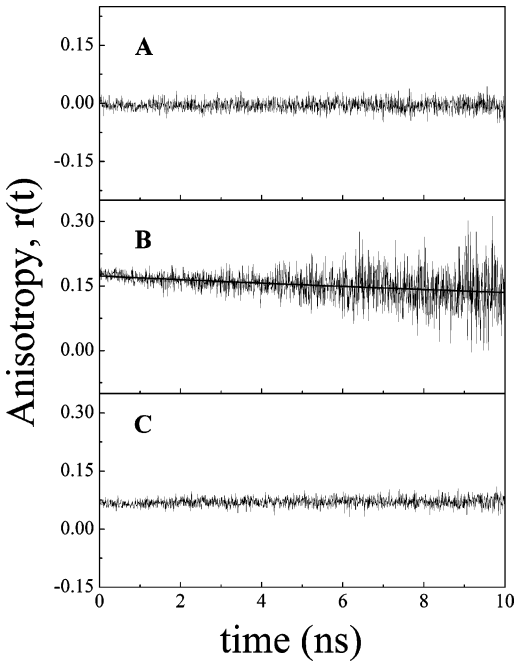

Figure 7. Anisotropy decays ($r(t)$) of (A) TPPC sodium salt in aqueous solution and (B) TPPC@Jeffamine in chloroform solution and (C) in aqueous solution. In the case of chloroform, also the curve fit (straight line) is plotted.

can be ascribed to a monomeric form of TPPC which is dominant in the presence of the polymer in aqueous solution, while the short-living fluorescent component can be assigned to nonmonomeric TPPC (small oligomers).[71] In chloroform solution, in the presence of polymer, the decay curve (Figure 6B) was fitted to three exponentials, whose lifetime and relative amplitudes are 2.6 ns (19%), 1.0 ns (17%), and 0.2 ns (64%). Maiti et al. reported a three-exponential behavior for the fluorescence emission of J-aggregates of tetrakis(4-sulfonatephenyl)porphyrin (TPPS) in buffer solution (pH = 3.5, [KCl] = 0.2 M) with lifetime values of 2.08, 0.29, and 0.05 ns.[29] Analogously, we can suggest that, in organic solvent, TPPC is present in the aggregated form.

Figure 7 shows the fluorescence anisotropy decays ($r(t)$) for the systems in the different solvents. In the case of free porphyrin in aqueous solution $r(t)$ is equal to zero (trace A). This fact can be probably due to the relative angle between the absorption and emission dipoles, which, in our conditions, could be close to the magic angle (54.7°), to which corresponds a fundamental anisotropy value (r_0) equal to zero. Indeed, a typical porphyrin molecule in aqueous solution exhibits a rotational correlation time (τ_R) of about 0.5 ns,[29] which is well within the time resolution of our instrumental apparatus. On the contrary, in the presence of polymer the r_0 values become 0.07 (in aqueous solution, trace C) and 0.17 (in chloroform, trace B), indicating that the porphyrin is interacting with Jeffamine molecules. Moreover, in both solvents the anisotropy decay times are very long: (i) in chloroform $r(t)$ is fitted as a single exponential with a rotational correlation time of about 40 ns; (ii) in aqueous solution the anisotropy decay appears as a plateau, indicating that the corresponding rotational correlation time is much longer than 40 ns. Maiti et al. reported a rotational correlation time of 10 ns for J-aggregate of TPPS in buffer solution, so that a τ_R value of 40 ns is much longer than expected in chloroform, whose viscosity is about 50% than water.[29] According to eq 4, the τ_R value measured in chloroform is compatible with a rotating unit of about 100−200 kDa mass, in line with porphyrin aggregates noncovalently bound to the polymer chains. On considering the molecular mass of a single TPPC@Jeffamine adduct (∼3200 Da), we estimate an aggregation number of more than 30 porphyrins in this organic solvent. On the other hand, in aqueous solution, all the spectroscopic evidence points to a predominant population of monomeric porphyrins interacting with the protonated Jeffamine chains. This basic unit undergoes to further aggregation yielding even larger clusters. Therefore, the very long rotational correlation time (≫40 ns) corresponding to a rotating unit with a molecular weight >100 kDa is consistent with a basic unit made by single monomeric TPPC molecules surrounded by four Jeffamine molecules, which then aggregates through the intermediacy of the poly(propylene oxide) side chains, leading to these larger aggregates. In these species, the direct interaction between adjacent porphyrin units is prevented by the presence of the Jeffamine chains.

The different behavior of the supramolecular adduct in the two solvent can be explained on the basis of the different extent of solvation of the two molecular components. In aqueous solution the anionic porphyrin is largely solubilized, and only a minor population of oligomers occurs. On the contrary, the poly(propylene oxide) moieties of the Jeffamine tend to avoid the interaction with the solvent by interdigitation and consequent clustering. Changes in the relative solubility in aqueous solutions have been also reported for porphyrins bearing poly(ethylene glycol) methyl ether chains covalently linked at the peripheral substituent groups. In this case, a consistent decrease of solubility with consequent aggregation has been observed for systems with low molecular mass (≤2100 Da).[72] On considering the higher hydrophobicity of poly(propylene oxide) with respect to poly(ethylene glycol), we expect that our supramolecular adduct undergoes easily monomer to aggregates equilibria. It is important to stress the point that even in these aggregated species the porphyrin core is embedded in the surrounding polymer chains, resulting in nonelectronically coupled chromophores. On the other hand, as evidenced by the time-resolved fluorescence measurements, the presence of Jeffamine moves the monomer−aggregate equilibrium toward TPPC in a monomeric form.

In organic solvent the anionic porphyrin tends to extensively self-aggregate because of the charge screening by tight ion-pairing among the carboxylate groups of TPPC and the protonated amino groups of the Jeffamine and the consequent increase of the van der Waals attractive contribution operating between the adjacent porphyrin cores. At the same time the polymer chains are well solvated and swelled in solutions, leading to more compact noninteracting aggregates. At difference with aqueous solutions, in chloroform the porphyrins are electronically coupled affording the observed changes in the corresponding spectroscopic features.

Small-Angle X-ray Scattering. To get more insights into the structure of this supramolecular system, SAXS measurements have been performed on quite concentrated aqueous solutions (2 and 20% w/w) at room temperature. Even if the concentration used in these experiments is at least an order of magnitude higher than for the spectroscopic measurements, important information on the nature of the basic unit can be extracted. Indeed, on the basis of the previously discussed experiments on time-resolved fluorescence anisotropy, we can reasonably assume in aqueous solution the coexistence of a population of large assemblies of TPPC@Jeffamine aggregated through the intermediacy of Jeffamine chains, together with monomeric TPPC@Jeffamine complexes. In the selected q range for the SAXS experiments the first aggregates are too large and

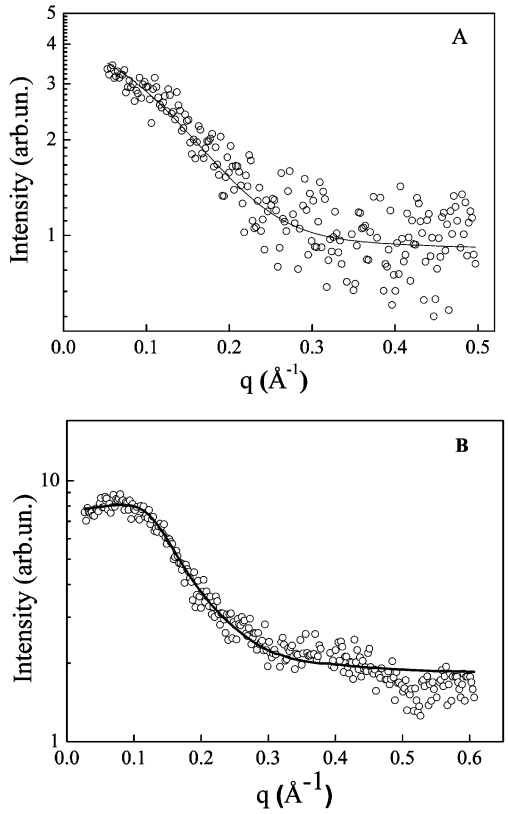

Figure 8. SAXS spectra of TPPC@Jeffamine (A) 2% w/w and (B) 20% w/w, at 298 K.

their scattered intensity is mainly lost in the forward direction, while an investigation at level of the monomeric building block remains possible. Therefore, on considering only this ensemble of monomers, the detected scattering intensity $I(q)$ in the SAXS experiment can be expressed as a product of the form factor $P(q)$, which contains information on the shape and dimension of the scattering particles, and the structure factor $S(q)$ describing the interparticle interaction:[65,66]

$$I(q) = N(\Delta\rho)^2 P(q) S(q) \tag{5}$$

where N is the number density of the micelles and $\Delta\rho = \rho - \rho_0$ is the so-called "contrast" (i.e., the difference between the scattering length density of the particle ρ and that of the solvent ρ_0). In the dilute region the interparticle interaction can be neglected (i.e., $S(q) \approx 1$), so that the analysis of scattering intensity $I(q)$ can afford direct information on morphological features of the scattering particles. Assuming our species as uniform spheres of radius R, the corresponding form factor $P(q)$ can be written as[65,66]

$$P(q) = [3J_1(qR)/(qR)]^2 = \left\{3\frac{[\sin(qR) - (qR)\cos(qR)]}{(qR)^3}\right\}^2 \tag{6}$$

where $J_1(x) = [\sin(x) - x\cos(x)]/x^2$ is the first-order spherical Bessel function.

This expression has been used to fit our data in the dilute regime, i.e., where interparticles interference effects are assumed to be negligible. A given polydispersity ΔR in the dimension of the scattering particles has been taken into account by introducing a Weibull-type distribution during the fitting procedure. Results of the fitting for the most diluted system investigated (2% w/w) is presented in Figure 8a. Scattering data are well reproduced in the whole q region and furnish a value of $R = 11.5 \pm 0.8$ Å for the TPPC@Jeffamine adduct. It is noteworthy that the low statistics in the scattering curves, especially at high q values, can be mainly related to the small dimensions of the scattering objects (the amount of scattered intensity is in fact proportional to the square of the particle volume) and further complicated by the low concentration of the sample. On increasing the concentration (20% w/w) a better statistics for the SAXS spectra has been achieved, while the interparticles interactions become progressively important (Figure 8b). In this case, the broad peak observable in the low-q region of the spectra is mainly connected to interparticles correlations.

The structure factor $S(q)$ of the system in eq 5 is estimated using the Percus−Yevick[73] approximation for the case of hard spheres (solid line in Figure 8b) in the Ornstein−Zernicke integral equation[74]

$$S(q) = \frac{1}{1 + 24\phi\dfrac{G(y,\phi)}{y}} \tag{7}$$

where ϕ is the volume fraction, $y = 2qR_{hs}$ (R_{hs} is the hard-sphere interaction radius), and $G(y,\phi)$ is a complex function of y and ϕ. The adopted potential takes into account excluded-volume interactions between interacting particles and can be considered as a first approximation of more complex potentials. It is important to observe that the average distance between particles calculated from the maximum of the structure factor $S(q)$ is $d = 38.9$ Å, which is near the close contact distance ($2R = 30.6$ Å). Furthermore, while the scattering data are well fitted in the low-q region, a sensitive discrepancy is detectable for higher q values of the spectra, where a bump is clearly detectable. This latter scattering features is probably connected with an internal interference caused by intraparticles contrast effects, and it may be indicative of a layered structure of the scattering objects. Accordingly, we can assume that the aggregates are composed by porphyrins in the core and polymer hydrophilic chains in a surrounding shell. The corresponding form factor can be described by a spherical core−shell model (Figure 9a) expressed as a function of core and shell radius, R_1 and R_2, respectively, and core and shell scattering length densities, ρ_c and ρ_s:[65,66]

$$P(q)(\Delta\rho)^2 = \left[\frac{4\pi}{3}R_1{}^3(\rho_c - \rho_s)\frac{3J_1(qR_1)}{qR_1} + \frac{4\pi}{3}R_2{}^3(\rho_s - \rho_0)\frac{3J_1(qR_2)}{qR_2}\right]^2 \tag{8}$$

Results obtained by fitting eq 8 to our SAXS data are presented in Figure 9b and clearly indicate how the main features of SAXS data are well reproduced by the adopted model in the whole q range explored. From the fitting procedure we obtain the values of $R_1 = 15.3$ Å for the core radius and the $R_2 = 21.8$ Å for the external radius of the particle. The obtained SAXS results clearly indicate that in aqueous solution the investigated samples form stable supramolecular species with a very small size. More specifically, the determined internal core radius is compatible with the porphyrin size (porphyrin average diameter is ~18 Å).

Conclusions

The simple interaction of the TPPC porphyrin in acid form with a stoichiometric amount of amino-terminated polymer leads to a supramolecular species behaving as a quite robust molecular

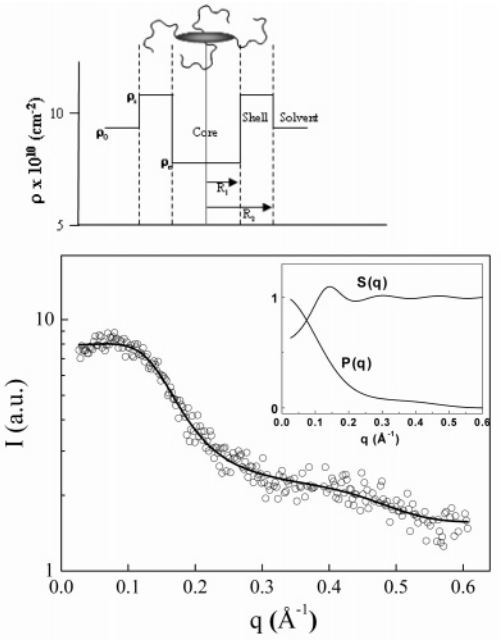

Figure 9. Schematic representation of the adopted core−shell model for the system form factor $P(q)$ (upper plot). Result of the fitting procedure for the sample 20% w/w. The corresponding form factor $P(q)$ and structure factor $S(q)$ are also reported in the inset.

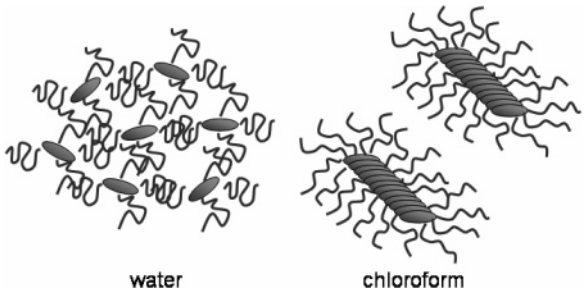

Figure 10. Pictorial sketch of the major species for the TPPC@Jeffamine adduct in aqueous and in chloroform solutions.

compound. The attractive electrostatic forces acting between the anionic carboxylate on the meso phenyl groups of the porphyrin and the protonated primary amino group of the polymer are mainly responsible for the stabilization of this species. In this framework, the solvent plays a very important role in driving different structural arrangements (Figure 10). In aqueous environment the Jeffamine exerts two different roles: (i) it enhances the solubility of the TPPC porphyrin, achieving unusually high concentration of the dye in solution (up to 60−80 mM), and (ii) it prevents extensive dimerization and further aggregation phenomena, which are commonly observed at much lower dye concentration in the absence of polymer. In this solvent the polymer chains, due to the partial hydrophobic character of the poly(propylene oxide), tend to assume a more compact conformation and to extensively self-aggregate, leading to large clusters. On the contrary, chloroform acts as a good solvent for the polymer chains which can swell in the solution. Ion-pairing is much more effective due to the dielectric constant of chloroform with respect to water; consequently, a more tight electrostatic interaction between oppositely charged species is expected. Anyway, screening of the overall charges on the single adducts can make the dispersive forces operative, leading to rather extensive porphyrin aggregation.

As the photophysical properties of porphyrins are widely modulated by their aggregation state, we expect that a fine-tuning of these properties can be achieved through a proper modulation of the overall structure. Our results suggest that this kind of supramolecular species can be exploited for the design of self-assembled systems to be employed in different fields, such as drug delivery and hybrid organic−inorganic materials for sensing or optical applications.

Acknowledgment. The authors thank the MIUR, COFIN 2004-2006, and CNR for financial support.

References and Notes

(1) Schenning, A.; Spelberg, J. H. L.; Driessen, M.; Hauser, M. J. B.; Feiters, M. C.; Nolte, R. J. M. *J. Am. Chem.* Soc. **1995**, *117*, 12655.
(2) Nolte, R. J. M. *FASEB J.* **1997**, *11*, A779.
(3) Tsuchida, E.; Komatsu, T.; Arai, K.; Yamada, K.; Nishide, H.; Bottcher, C.; Fuhrhop, J. H. *J. Chem. Soc., Chem. Commun.* **1995**, 1063.
(4) Pasternack, R. F.; Gibbs, E. J. Porphyrin and metalloporphyrin interactions with nucleic acids. In *Metal Ions in Biological Systems*; Marcel Dekker: New York, 1996; Vol. 33, p 367.
(5) Scolaro, L. M.; Romeo, A.; Pasternack, R. F. *J. Am. Chem. Soc.* **2004**, *126*, 7178.
(6) Mukundan, N. E.; Petho, G.; Dixon, D. W.; Marzilli, L. G. *Inorg. Chem.* **1995**, *34*, 3677.
(7) Pasternack, R. F.; Brigandi, R. A.; Abrams, M. J.; Williams, A. P.; Gibbs, E. J. *Inorg. Chem.* **1990**, *29*, 4483.
(8) Pasternack, R. F.; Goldsmith, J. I.; Szep, S.; Gibbs, E. J. *Biophys. J.* **1998**, *75*, 1024.
(9) Bellacchio, E.; Lauceri, R.; Gurrieri, S.; Scolaro, L. M.; Romeo, A.; Purrello, R. *J. Am. Chem. Soc.* **1998**, *120*, 12353.
(10) Pancoska, P.; Urbanova, M.; Bednarova, L.; Vacek, K.; Paschenko, V. Z.; Vasiliev, S.; Malon, P.; Kral, M. *Chem. Phys.* **1990**, *147*, 401.
(11) Nezu, T.; Ikeda, S. *Bull. Chem. Soc. Jpn.* **1993**, *66*, 25.
(12) Pasternack, R. F.; Gibbs, E. J. *J. Inorg. Organomet. Polym.* **1993**, *3*, 77.
(13) Purrello, R.; Bellacchio, E.; Gurrieri, S.; Lauceri, R.; Raudino, A.; Scolaro, L. M.; Santoro, A. M. *J. Phys. Chem. B* **1998**, *102*, 8852.
(14) Purrello, R.; Raudino, A.; Scolaro, L. M.; Loisi, A.; Bellacchio, E.; Lauceri, R. *J. Phys. Chem. B* **2000**, *104*, 10900.
(15) Purrello, R.; Scolaro, L. M.; Bellacchio, E.; Gurrieri, S.; Romeo, A. *Inorg. Chem.* **1998**, *37*, 3647.
(16) Borissevitch, I. E.; Tominaga, T. T.; Imasato, H.; Tabak, M. *Anal. Chim. Acta* **1997**, *343*, 281.
(17) Borissevitch, I. E.; Tominaga, T. T.; Imasato, H.; Tabak, M. *J. Lumin.* **1996**, *69*, 65.
(18) Pandey, R. K.; Zheng, G. Porphyrins as Photosensitizers in Photodynamic Therapy. In *The Porphyrin Handbook*; Kadish, K. M., Smith, K. M., Guilard, R., Eds.; Academic Press: New York, 2000; Vol. 6, p 157.
(19) White, W. I. In *The Porphyrins*; Dolphin, D., Ed.; Academic Press: New York, 1978; Vol. 5, p 303.
(20) Scolaro, L. M.; Castriciano, M.; Romeo, A.; Mazzaglia, A.; Mallamace, F.; Micali, N. *Physica A* **2002**, *304*, 158.
(21) Micali, N.; Villari, V.; Scolaro, L. M.; Romeo, A.; Castriciano, M. A. *Phys. Rev. E* **2005**, *72*.
(22) Mallamace, F.; Micali, N.; Trusso, S.; Scolaro, L. M.; Romeo, A.; Terracina, A.; Pasternack, R. F. *Phys. Rev. Lett.* **1996**, *76*, 4741.
(23) Mallamace, F.; Scolaro, L. M.; Romeo, A.; Micali, N. B. *Phys. Rev. Lett.* **1999**, *82*, 3480.
(24) McRae, E. G.; Kasha, M. *J. Chem. Phys.* **1958**, *28*, 721.
(25) McRae, E. G.; Kasha, M. In *Physical Processes in Radiation Biology*; Augenstein, L., Mason, R., Rosenberg, B., Eds.; Academic Press: New York, 1964; p 23.
(26) Gandini, S. C. M.; Gelamo, E. L.; Itri, R.; Tabak, M. *Biophys. J.* **2003**, *85*, 1259.
(27) Akins, D. L.; Zhu, H. R.; Guo, C. *J. Phys. Chem.* **1994**, *98*, 3612.
(28) Castriciano, M.; Romeo, A.; Villari, V.; Micali, N.; Scolaro, L. M. *J. Phys. Chem. B* **2003**, *107*, 8765.
(29) Maiti, N. C.; Ravikanth, M.; Mazumdar, S.; Periasamy, N. *J. Phys. Chem.* **1995**, *99*, 17192.
(30) Ohno, O.; Kaizu, Y.; Kobayashi, H. *J. Chem. Phys.* **1993**, *99*, 4128.
(31) Pasternack, R. F.; Schaefer, K. F.; Hambright, P. *Inorg. Chem.* **1994**, *33*, 2062.
(32) Ribo, J. M.; Crusats, J.; Farrera, J. A.; Valero, M. L. *J. Chem. Soc., Chem. Commun.* **1994**, 681.
(33) Rotomskis, R.; Augulis, R.; Snitka, V.; Valiokas, R.; Liedberg, B. *J. Phys. Chem. B* **2004**, *108*, 2833.
(34) Schwab, A. D.; Smith, D. E.; Rich, C. S.; Young, E. R.; Smith, W. F.; de Paula, J. C. *J. Phys. Chem. B* **2003**, *107*, 11339.
(35) Collini, E.; Ferrante, C.; Bozio, R. *J. Phys. Chem. B* **2005**, *109*, 2.

(36) Schwab, A. D.; Smith, D. E.; Bond-Watts, B.; Johnston, D. E.; Hone, J.; Johnson, A. T.; de Paula, J. C.; Smith, W. F. *Nano Lett.* **2004**, *4*, 1261.
(37) Clarke, S. E.; Wamser, C. C.; Bell, H. E. *J. Phys. Chem. A* **2002**, *106*, 3235.
(38) Choi, M. Y.; Pollard, J. A.; Webb, M. A.; McHale, J. L. *J. Am. Chem. Soc.* **2003**, *125*, 810.
(39) Doan, S. C.; Shanmugham, S.; Aston, D. E.; McHale, J. L. *J. Am. Chem. Soc.* **2005**, *127*, 5885.
(40) Pasternack, R. F.; Huber, P. R.; Boyd, P.; Engasser, G.; Francesconi, L.; Gibbs, E.; Fasella, P.; Cerio Venturo, G.; Hinds, L. d. *J. Am. Chem. Soc.* **1972**, *94*, 4511.
(41) Khairutdinov, R. F.; Serpone, N. *J. Phys. Chem. B* **1999**, *103*, 761.
(42) Maiti, N. C.; Mazumdar, S.; Periasamy, N. *J. Phys. Chem. B* **1998**, *102*, 1528.
(43) Cherian, S.; Wamser, C. C. *J. Phys. Chem. B* **2000**, *104*, 3624.
(44) For applications see www.biomoda.com.
(45) Swarts, J. C.; Neuse, E. W.; Perlwitz, A. G.; Stephanou, A.; Lamprecht, G. J. *Angew. Makromol. Chem.* **1993**, *207*, 123.
(46) Chiba, U.; Neuse, E. W.; Swarts, J. C.; Lamprecht, G. J. *Angew. Makromol. Chem.* **1994**, *214*, 137.
(47) Yue, Z. L.; Eccleston, M. E.; Slater, N. K. H. *Biomaterials* **2005**, *26*, 6357.
(48) Marie, E.; Landfester, K.; Antonietti, M. *Biomacromolecules* **2002**, *3*, 475.
(49) Yuan, J.; Zhu, J.; Zhu, C. H.; Shen, J.; Lin, S. C. *Polym. Int.* **2004**, *53*, 1722.
(50) Everaerts, F.; Torrianni, M.; van Luyn, M.; van Wachem, P.; Feijen, J.; Hendriks, M. *Biomaterials* **2004**, *25*, 5523.
(51) Chen, R. J.; Yue, Z. L.; Eccleston, M. E.; Williams, S.; Slater, N. K. H. *J. Controlled Release* **2005**, *108*, 63.
(52) Kuznetsov, Y. G.; Malkin, A. J.; McPherson, A. *J. Cryst. Growth* **2001**, *232*, 30.
(53) Chen, G. H.; Vanderdoes, L.; Bantjes, A. *J. Appl. Polym. Sci.* **1993**, *48*, 1189.
(54) Park, I.; Wang, Z.; Pinnavaia, T. J. *Chem. Mater.* **2005**, *17*, 383.
(55) Jordens, K.; Wilkes, G. *J. Macromol. Sci., Pure Appl. Chem.* **2000**, *37*, 815.
(56) Cai, Y. L.; Tang, Y. Q.; Armes, S. P. *Macromolecules* **2004**, *37*, 9728.
(57) Sannier, L.; Siddiqi, H. M.; Dumon, M.; Gyselinck, F.; Maschke, U. *Mol. Cryst. Liq. Cryst.* **2001**, *367*, 3055.
(58) Wang, Z.; Pinnavaia, T. J. *J. Mater. Chem.* **2003**, *13*, 2127.
(59) Lin, J. J.; Cuscurida, M.; Waddill, H. G. *Ind. Eng. Chem. Res.* **1997**, *36*, 1944.
(60) Pasternack, R. F.; Collings, P. J. *Science* **1995**, *269*, 935.
(61) O'Connor, D. V.; Phillips, D. *Time-Correlated Single Photon Counting*; Academic Press: New York, 1984.
(62) Castriciano, M. A.; Romeo, A.; Villari, V.; Angelini, N.; Micali, N.; Scolaro, L. M. *J. Phys. Chem. B* **2005**, *109*, 12086.
(63) Marquadt, D. W. *J. Soc. Ind. Appl. Math.* **1969**, *11*, 431.
(64) Lakowicz, J. R. *Principles of Fluorescence Spectroscopy*; Kluwer Academic/Plenum Publishers: New York, 1999.
(65) Feign, L. A.; Svergun, D. I. *Structure Analysis by Small-Angle X-ray and Neutron Scattering*; Plenum Press: New York, 1987.
(66) Glatter, O.; Kratky, O. *Small-Angle X-ray Scattering*; Academic Press: London, 1982.
(67) Strobl, G. *Acta Crystallogr.* **1970**, *A26*, 367.
(68) Kano, K.; Minamizono, H.; Kitae, T.; Negi, S. *J. Phys. Chem. A* **1997**, *101*, 6118.
(69) Gouterman, M. *Optical Spectra and Electronic Structure of Porphyrins and Related Rings*; Academic Press: New York, 1978; Vol. 3.
(70) Parkash, J.; Robblee, J. H.; Agnew, J.; Gibbs, E.; Collings, P.; Pasternack, R. F.; de Paula, J. C. *Biophys. J.* **1998**, *74*, 2089.
(71) It is important to note that, in the steady-state fluorescence spectrum (which is time-integrated), the contribution of each fluorescent component to the total emission is proportional to the product $\alpha \times \tau$ (see eq 1). Under this assumption, in our experimental conditions, the steady-state fluorescence measurements in aqueous solution take essentially into account only the long-living fluorescent species, being the contribution of the short-living ones about 4%.
(72) Micali, N.; Villari, V.; Mineo, P.; Vitalini, D.; Scamporrino, E.; Crupi, V.; Majolino, D.; Migliardo, P.; Venuti, V. *J. Phys. Chem. B* **2003**, *107*, 5095.
(73) Percus, J. K.; Yevick, G. J. *Phys. Rev.* **1958**, *110*, 1.
(74) Hansen, J. P.; McDonald, I. R. *Theory of Simple Liquids*; Academic Press: London, 1986.

MA060583I